ISSN 1063-7737, Astronomy Letters, 2019, Vol. 45, No. 1, pp. 1–9. © Pleiades Publishing, Inc., 2019.
Russian Text © K.S. Strigunov, A.V. Zhovtan, Yu.I. Neshpor, G.A. Borman, 2019, published in Pis'ma v Astronomicheskii Zhurnal, 2019, Vol. 45, No. 1, pp. 3–12.

Long-Term Observations of the Blazar Mrk 501 with the GT-48 Cherenkov Telescope

K. S. Strigunov[1*], A. V. Zhovtan[1], Yu. I. Neshpor[1***], and G. A. Borman[1****]**

[1] *Crimean Astrophysical Observatory, pos. Nauchnyi, Crimea, 298409 Russia*

Received August 4, 2017; revised June 20, 2018; accepted September 4, 2018

Abstract—The galaxy Mrk 501 has been monitored with the GT-48 Cherenkov telescope at the Crimean Astrophysical Observatory for 14 years (1997–2010). Very-high-energy (VHE) gamma-ray photons have been recorded from Mrk 501 with a total significance of 15σ. The arrival directions of VHE gamma-ray photons have been mapped. They have been identified with Mrk 501. The TeV fluxes from Mrk 501 are shown to be highly variable. The light curves from the data of Cherenkov telescopes and the telescopes that observed Mrk 501 at high energies (MeV and GeV) and in the X-ray and optical bands are presented. Based on the GT-48 observations, we have constructed a TeV spectrum and determined the differential spectral index. The fluxes and spectral characteristics of Mrk 501 inferred from the GT-48 observations are consistent with the data of the MAGIC and H.E.S.S. Collaborations, respectively.

DOI: 10.1134/S1063773719010043

Keywords: *gamma-ray photons, Cherenkov telescope, active galactic nuclei, blazar.*

1. INTRODUCTION

The studies of active galactic nuclei (AGNs) at very high energies (VHE) $E > 10^{11}$ eV by means of ground-based gamma-ray astronomy were begun in the 1990s with the launch of the Compton Gamma-Ray Observatory (CGRO), which discovered gamma rays with energies $E > 100$ MeV from a number of AGNs. These objects arouse enormous interest from an astrophysical point of view. They exhibit significant flux variations in the entire frequency range, from radio to VHE gamma-ray emission. The variation time scale changes from days to a year. AGNs are distinguished by a strong tendency for flare (a time scale of several days) and explosive (a duration of several months) activity. The galaxies Mrk 501 and Mrk 421 were the first to be detected among AGNs in the VHE gamma-ray range (Quinn et al. 1996). At the Crimean Astrophysical Observatory (CrAO) gamma-ray emission from the AGN Mrk 501 was recorded in 1997 at the GT-48 Cherenkov telescope with a high significance: 11 standard deviations (Kalekin et al. 1999). VHE gamma-ray variability from night to night was detected in the 1997 data.

*E-mail: sks6891@gmail.com
**E-mail: astroalex2012@gmail.com
***E-mail: yuri.neshpor@gmail.com
****E-mail: borman.ga@gmail.com

2. LONG-TERM GT-48 OBSERVATIONS OF THE OBJECT Mrk 501

The AGN Mrk 501 (the coordinates for 2000: $\alpha = 16^{\rm h}53^{\rm m}53^{\rm s}$ and $\delta = 39°45'32''$) was observed at CrAO from 1997 to 2010 inclusive with the GT-48 telescope. The GT-48 Cherenkov telescope (for an image of GT-48, see the site of the CrAO Department of Extragalactic Research and Gamma-Ray Astronomy[1]) is located at an altitude of 600 m above sea level and consists of two identical alt-azimuth mountings, northern and southern. They are spaced 20 m apart in the north–south direction. There are six telescopes (elements) on each mounting. The optics of each element consists of four mirrors (1.2 m in diameter) with a common focus. The total area of the mirrors is 54 m^2. After aluminizing, which is done every four years, the reflectivity is 0.95. The reflecting layer is deposited and fixed by anode oxidation. The mirrors of four elements have a focal length of 5 m. They are designed to record optical emission in the range 300–550 nm. The field of view of the telescopes (the field of view of the telescope camera) is 2.8°. There is a camera in the focal plane of the mirrors of each element. The camera consists of 37 photomultiplier tubes (PMT-140). The images of Cherenkov flashes are recorded with them. There is a conical optical fiber in front of each PMT. Their application allows the flux utilization factor to be increased to 90%. Two

[1] http://lerga.craocrimea.ru/Instr/gt48_ru.html

other elements have a focal length of 3.2 m. They are designed to record ultraviolet (UV) emission in the range 200–300 nm. In each section there are elements combined into four 1.2-m mirrors; UV detectors, which are solar-blind PMTs with their sensitivity peak in the soft UV range (~270 nm), are mounted at their focus. UV emission is recorded as an additional parameter (selection criterion), based on which it is also possible to separate the γ-ray and p-showers by estimating the relative contribution of the UV emission to the total flux. The GT-48 threshold energy is 1 TeV. The operating range is 1–70 TeV. The energy resolution is ~0.5 TeV. The operating range was determined as follows. The threshold energy (i.e., the lower boundary of the range) of 1 TeV is an effective energy threshold defined as the energy above which 95% of all events are recorded. The upper boundary means that at energies above 70 TeV it is impossible to obtain a response of the instrumentation and to extract the signal from noise, because the gamma-ray flux is $\sim 10^{-13}$–10^{-14} photon cm^{-2} s^{-1} or lower. Below we give a clarification: the 0.5-TeV resolution is not retained with increasing energy, i.e., this is the maximum resolution corresponding to energies near 1 TeV. The resolution decreases with increasing energy and, accordingly, decreasing flux: the resolution is ~0.5, ~1, ~7, and ~20 TeV in the energy ranges 1–4, 5–15, 15–40, and >40 TeV, respectively. With the available GT-48 data statistics it is virtually impossible to separate the fluxes in subbands less than 0.5 TeV (for example, from 1 to 1.2 TeV, i.e., 0.2 TeV) due to significant errors. In other ranges, with higher energies, the resolution deteriorates due to a reduction in the gamma-ray flux. Therefore, for a reliable determination of the gamma-ray flux we have to extend the subband boundaries—only in this way does it become possible to obtain a statistically significant result. The gamma-ray flux at TeV energies from the Crab Nebula with a significance $>5\sigma$ can be detected with the GT-48 telescope in 8.5 h of observations (Kalekin et al. 1995). The accuracy of determining the primary particle arrival direction is 0.2°.

VHE gamma-ray photons do not reach the Earth's surface. However, they interact with the nuclei of air atoms to produce extensive air showers (EASs). EASs consist of high-energy electrons and positrons. Charged EAS particles emit Cherenkov photons at a small angle (~1°) to the propagation direction of the primary gamma-ray photon (γ-ray flash). This allows them to be recorded and the direction to their source to be determined. At the same time, charged cosmic-ray particles (background) also produce Cherenkov flashes (p-flashes) in the Earth's atmosphere. They differ little from γ-ray flashes and therein lies the main problem of their selection. Nevertheless, there are differences. The camera multichannel detectors allow the overwhelming majority of p-flashes to be separated.

The observations were carried out by the two sections in the object tracking mode. The events that were observed simultaneously on both sections were recorded. Each session included the on-source observations $N_{\rm on}$ (25 min) by the tracking method and separately the off-source observations $N_{\rm off}$ (25 min). The number of events (Cherenkov flashes) during the on-source observations include the events from the source plus the events from the background ($N_{\rm on}$). Only the events from cosmic rays $N_{\rm off}$ are recorded during the off-source observations. The duration of the GT-48 observations $N_{\rm on}$ and $N_{\rm off}$ is the same and was determined from a quartz clock with an accuracy of 10^{-3} s. These observations were carried out at the same zenith and azimuth angles. As a result, 441 observing sessions were conducted. The number of hours of Mrk 501 (on-source) observations over all years of observations was more than 180 h. The systematic effects were taken into account using the calibration from Vladimirskii et al. (1995). The calibration is performed after each observing session. A pulsed molecular nitrogen gas laser was used for the calibration. The pulse duration is 15 ns. The light beam for uniform illumination of the entire area is transmitted with an optical fiber. As a result, with the calibration coefficients the sensitivity of each of the 37 channels was the same. The events in which the analog-to-digital converter was saturated at least in one of the channels were also attributed to the systematic effects. The flashes whose maximum amplitude was in the outer ring of the detector cells were attributed to the systematic effects, because for such flashes it is impossible to determine their sizes. The dispersion of the count rates of Cherenkov flashes in each of the observing sessions was also taken into account. All these effects were taken into account during the primary data reduction. In addition, only those observations that were carried out under favorable constant weather conditions were used for the data reduction. Note that the observations of objects are carried out in the range of zenith angles from 0° to 30° (for Mrk 501 from 6° to 30°). The angular distance between the on- and off-source observation regions was 7.5°.

The data obtained were subjected to further reduction needed to analyze the digital images of flashes. Mathematical methods were used for this purpose. The first and second moments of the light distribution were calculated. The parameters of each Cherenkov flash were found from them, which are divided into two types. The parameters that do not depend on the source position relative to the telescope camera center (coordinate-independent parameters) belong

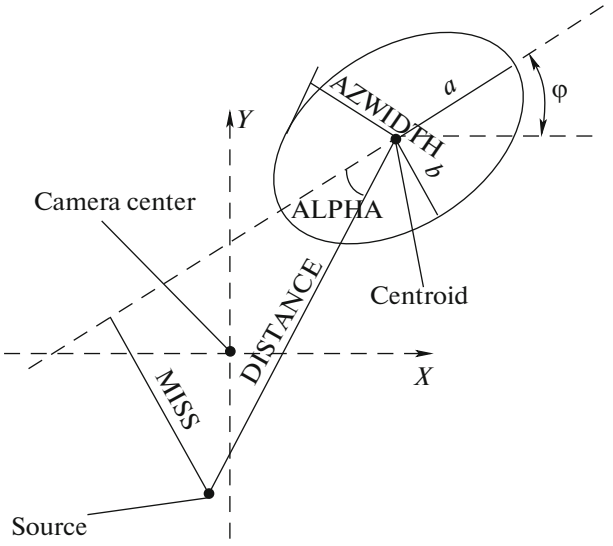

Fig. 1. Schematic view of some Cherenkov flash parameters presented in the form of an ellipse. The semimajor axis of the ellipse a is LENGTH; the semiminor axis of the ellipse b is WIDTH; DISTANCE is the angular distance between the flash center and the source; ALPHA is the angle between the flash major axis and the straight line connecting the flash center and the source position relative to the telescope camera center; MISS is the smallest distance between the flash major axis and the source; AZWIDTH is the azimuthal width; φ is the flash position angle characterizing the direction of its maximum elongation, i.e., its orientation.

to the first type. The parameters that depend on the source position relative to the telescope camera center (coordinate-dependent parameters) belong to the second type. These parameters are described in detail in Vladimirskii et al. (1995). Up to 99% of the off-source events can be rejected using the differences between the images of γ-ray and p-flashes. A schematic view of a flash and some of its parameters are shown in Fig. 1. The coordinate-dependent selection criteria are most efficient. The quantity that characterizes the selection efficiency is denoted by Q and calculated from the formula

$$Q = \frac{N_\gamma/\sqrt{N_p}}{N_{\gamma 0}/\sqrt{N_{p0}}}, \qquad (1)$$

where $N_{\gamma 0}$ and N_{p0} are the numbers of showers before the selection, N_γ and N_p are the numbers of showers after the selection. The selection efficiency Q is the factor by which the selection increases the sensitivity of the Cherenkov telescope: in a fixed time the telescope will detect a factor of Q fainter gamma-ray flux from the object. At a constant flux from the source the detection time decreases by a factor of Q^2. The coordinate-dependent flash parameters (for them Q is 3–4) belong to the most efficient criteria. It should be noted that a number of parameters are used simultaneously during the selection, which increases its efficiency.

Table 1 shows $N_{\rm on}$ and $N_{\rm off}$ in a time interval Δt during the Mrk 501 observations; n is the number of recorded VHE gamma-ray photons in 1 min; σ is the significance of the recorded VHE gamma-ray flux, which is determined from the Li–Ma formula (Li and Ma 1983)

$$S = \frac{N_{\rm on} - N_{\rm off}}{\sqrt{N_{\rm on} + N_{\rm off}}}, \qquad (2)$$

where $N_{\rm on}$ is the number of on- and off-source events, $N_{\rm off}$ is the number of off-source events.

The boundary values of the selection parameters were chosen in such a way as to obtain the gamma-ray flux with the greatest significance. In this case, we applied simultaneously several selection parameters: we used the coordinate-independent parameters (A and B, i.e., the major and minor axes of the flash, respectively, because A and B are the most efficient coordinate-independent parameters) and coordinate-dependent parameters (mostly ALPHA, AZWIDTH, and MISS, because they are the most efficient coordinate-dependent parameters). Applying one of the parameters rejects only a small fraction of p-showers (background), because the γ-ray and p-showers are similar between themselves. However, applying a combination of parameters allows the fraction of the rejected cosmic-ray background to be increased significantly; R is the rejection coefficient, i.e., the factor by which the relative fraction of gamma-ray showers in the selected data set is higher than that in the original one (the data without selection):

$$R = \frac{N_\gamma/N_p}{N_{\gamma 0}/N_{p0}}, \qquad (3)$$

where $N_{\gamma 0}$ and N_{p0} are the numbers of showers before the selection, N_γ and N_p are the numbers of showers after the selection. Note that with the coordinate-dependent parameters the rejection efficiency of off-source events is higher that that with the coordinate-independent parameters (A and B). The efficiency increases sharply when not only the parameters A and B are used in the selection, but also the coordinate-dependent parameters (in our case, ALPHA, AZWIDTH, and MISS) are added. Table 2 shows the boundary values of the parameters in the combination with which the gamma-ray photon count rates were obtained for Mrk 501 with the greatest significance in each of the years (the parameters A and B plus the coordinate-dependent parameter the selection by which yielded the most significant result) that correspond to the yearly mean count rates in Table 1 and the rejection coefficient R.

Table 1. Results of our long-term observations of Mrk 501 with GT-48

Year	Intervals of observations (days and months)	N_{on}	N_{off}	Δt, min	n, min^{-1}	σ	Flux, $\times 10^{-12}$ photon cm^{-2} s^{-1}
1997	May 1–June 10	30 139	29 342	1150	0.381 ± 0.032	11.7	32.1 ± 4.6
1998	May 26–Aug. 23	18 031	17 713	850	0.234 ± 0.040	5.9	25.3 ± 7.5
2000	June 24–July 30	12 676	12 178	575	0.148 ± 0.034	4.4	22.7 ± 4.8
2002	May 13–July 16	9400	9449	625	0.075 ± 0.025	2.9	11.6 ± 6.0
2003	Apr. 28–July 6	20 863	20 475	1475	0.227 ± 0.047	4.8	21.2 ± 10.6
2004	May 18–July 22	14 461	13 991	1100	0.095 ± 0.019	5.0	12.3 ± 4.3
2006	May 23–Jun 26	6601	6292	450	0.308 ± 0.057	5.4	29.5 ± 8.2
2007	June 5–Aug. 20	25 730	25 197	1450	0.055 ± 0.012	4.5	3.7 ± 2.3
2008	June 1–Aug. 8	19 311	19 122	1175	0.157 ± 0.035	4.4	14.4 ± 4.9
2009	May 18–July 29	16 581	17 091	1350	0.053 ± 0.010	5.1	10.7 ± 3.3
2010	May 13–July 19	6909	7057	825	0.076 ± 0.017	4.4	4.0 ± 1.3

We constructed the distribution in one of the coordinate-dependent selection parameters for Mrk 501 (Fig. 2). The presented distribution in ALPHA shows that the selection efficiency for Mrk 501 increased at ALPHA (the angle between the flash major axis and the straight line connecting the flash center and the source position relative to the telescope camera center) less than 25° and the number of on-source plus off-source events (ON-data) exceeded considerably the number of off-source events (OFF-data). In the case of selection by ALPHA in Fig. 2, the number of on-source events in the most significant result exceeded the number of off-source events by 213 events.

Note that the coordinate-dependent parameters (as an example, we showed the distribution in ALPHA, because it is one of the efficient selection criteria) make a major contribution to the rejection of the cosmic-ray background (p-showers), but with the selection by A and B. For Mrk 501 their boundary values were $<0.3°$ and $<0.18°$, respectively. However, since the coordinate-dependent parameter ALPHA makes the greatest contribution to the selection, the distribution was constructed precisely in this parameter. Here we emphasize: we obtained the most significant yearly mean results in different years not only from ALPHA, but it will suffice to construct the distribution only in one of the coordinate-dependent parameters (with A and B, see above) over all years (when the data were reduced not over individual years, but the entire data set was reduced over all years).

3. LOCALIZATION OF THE VHE GAMMA-RAY SOURCE Mrk 501

The multichannel detectors of second-generation gamma-ray telescopes allow the region on the celestial sphere in which the gamma-ray source is located to be refined. The trial source method (Akerlof et al. 1991; Fomin et al. 1994; Neshpor et al. 1994) is applied for this purpose. The method is based on the fact that the images of the flashes from gamma-ray photons are oriented in the telescope focal plane toward the source, while the major axes of the el-

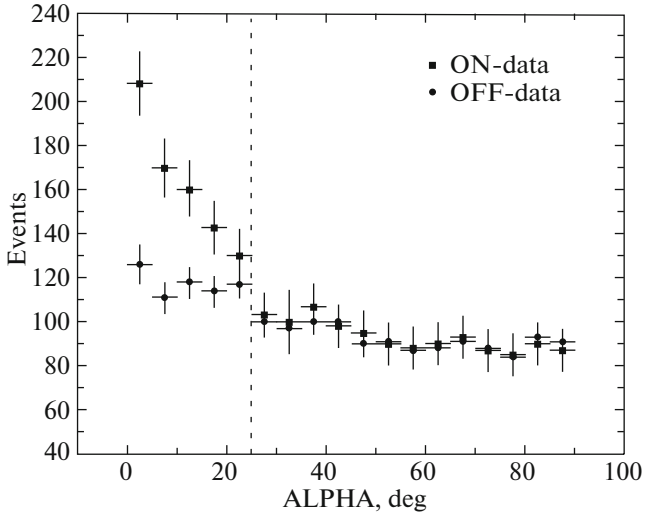

Fig. 2. Distribution of the number of events in parameter ALPHA for Mrk 501. ON-data denotes the number of on-source and off-source events, OFF-data denotes the number of off-source events.

Table 2. Selection parameters and rejection coefficients

Years	Mrk 501		
	parameters	values, deg	rejection coefficient, R
1997	A	<0.30	
	B	<0.15	17.9
	ALPHA	<27.0	
1998	A	<0.29	
	B	<0.17	19.5
	ALPHA	<30.0	
2000	A	<0.31	
	B	<0.20	11.3
	MISS	<0.22	
2002	A	<0.31	
	B	<0.18	76.1
	MISS	<0.19	
2003	A	<0.35	
	B	<0.22	12.5
	MISS	<0.21	
2004	A	<0.32	
	B	<0.19	16.5
	ALPHA	<31.0	
2006	A	<0.33	
	B	<0.21	7.8
	AZWIDTH	<0.24	
2007	A	<0.25	
	B	<0.19	24.1
	ALPHA	<23.0	
2008	A	<0.30	
	B	<0.16	21.0
	MISS	<0.15	
2009	A	<0.32	
	B	<0.25	24.0
	AZWIDTH	<0.23	
2010	A	<0.26	
	B	<0.19	29.0
	AZWIDTH	<0.19	

lipses of the flashes initiated by cosmic rays, to a first approximation, are oriented uniformly in all directions. Therefore, if we select the flashes by taking an arbitrary point (the so-called trial source) in the focal plane with coordinates (X_iY_j) as the direction to the source and apply the selection by coordinate-dependent parameters, then the number of selected proton showers will not depend on the position of the presumed source, while the number of selected gamma-ray photons will have a maximum when the presumed source coincides with the true one. The field of view of the telescope camera is 2.8°. It is broken down into a grid with a 0.1° step. Trial sources are specified at the grid points. After processing the available data set according to a particular coordinate-dependent selection criterion, we obtain a file with three columns: the first gives the deviations from the camera center in right ascension, the second gives the deviations in declination, and the third gives the number of events. The deviation step is 0.1°. Using the selection parameters, we constructed a three-dimensional histogram of selected events from the on-source and background observations $N_{\rm on}$. The histogram constructed for the background $N_{\rm off}$ was subtracted from the histogram $N_{\rm on}$. The final histogram shows the distribution of γ-ray flashes over the camera field of view with the maximum number of γ-ray flashes toward the gamma-ray source (Fig. 3).

Based on the three-dimensional image (Fig. 3), we also constructed the isophotes (Fig. 4). The maximum of the distribution occurs at the camera center coincident with the Mrk 501 position. The numbers of events are shown in the upper right corner. The maximum values correspond to the direction to the gamma-ray source.

4. THE ACTIVITY OF Mrk 501 IN VARIOUS RANGES. THE TeV SPECTRUM OF Mrk 501

Table 1 presents the yearly mean results of our Mrk 501 observations in count rates. They were obtained with the GT-48 Cherenkov telescope in the period from 1997 to 2010 inclusive. VHE gamma-ray photons were recorded from Mrk 501 with a total significance of 15σ. In addition, the yearly mean fluxes from Mrk 501 in the period from 1997 to 2010 inclusive are presented. The VHE emission is seen to vary from year to year, while the most powerful perturbation occurred in 1997.

Furthermore, this object was also observed in other ranges. In particular, Mrk 501 was observed in the optical band at CrAO in the period from 1997 to 2011 with the AZT-8 telescope (for an image of the telescope, see the site of the CrAO Department of Extragalactic Research and Gamma-Ray Astronomy[2]).

[2] http://lerga.craocrimea.ru/Instr/azt8_ru.html

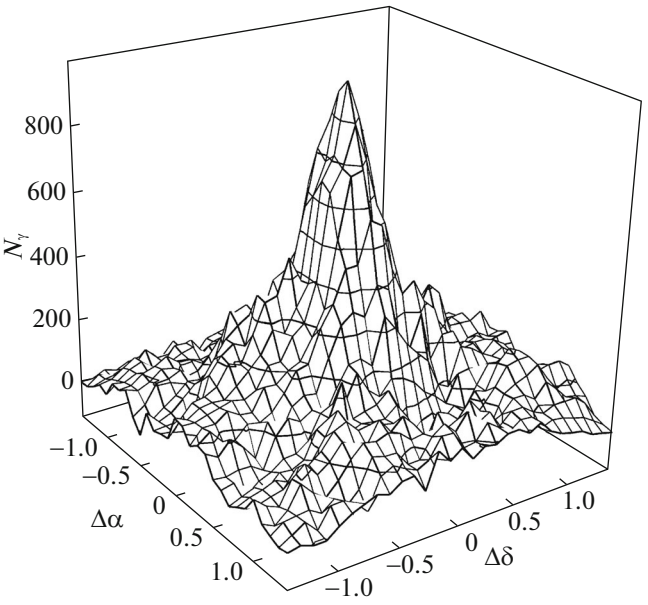

Fig. 3. Three-dimensional histogram of the selected gamma-ray events (N_γ) over the detector field of view. $\Delta\delta$ is the deviation from the position of the telescope camera center in declination (in deg). $\Delta\alpha$ is the deviation in right ascension (in deg). The image was constructed using the selection for Mrk 501 over all years of observations.

The two-mirror AZT-8 telescope was manufactured by the Leningrad Optical Mechanical Association (LOMO) in 1964. The optical system of the telescope is Cassegrain. It consists of a primary parabolic mirror ($D = 70$ cm, $F = 282$ cm) with a relative aperture of F/4 and two secondary mirrors that form Cassegrain foci of F/16 and F/40 with field of views from 40 to 18 arcmin. The prime focus provides a field of view ∼10 arcmin. The AZT-8 mounting is equatorial. The detector is a BVRI photometer based on an Apogee AP7p CCD camera. An aperture of 15 arcsec was used for photometry. More detailed information about the AZT-8 telescope is accessible at the site of the CrAO Department of Extragalactic Research and Gamma-Ray Astronomy. The data in other bands, including those in the optical one, are presented in Fig. 5. The optical light curve was constructed from the B-band (with an effective wavelength of 4330 Å) observations with the AZT-8 telescope (CrAO). The X-ray data were taken from the RXTE/ASM[3] and Swift/BAT[4] observations (the 2–10 and 15–50 keV bands, respectively). The data in the range 0.1–300 GeV were taken from the second Fermi catalogue (2FGL[5]), where the Fermi LAT observations are provided. The fluxes in the range 0.1–300 GeV were averaged over 30 days. Finally, the VHE light curves of Mrk 501 observed with different Cherenkov telescopes, including GT-48, were presented. The mean flux at energies >1 TeV over all years of observations with GT-48 (1997–2010) for Mrk 501 was $(9.7 \pm 0.9) \times 10^{-12}$ photon cm^{-2} s^{-1}. The CAT (>250 GeV), HEGRA CT1 (>1.5 TeV), and MAGIC (>1 TeV) data were taken from Albert et al. (2007). The VERITAS (>300 GeV) data were taken from Huang and Konopelko (2009) and Aleksic et al. (2015). The Whipple (>350 GeV) data were taken at the site[6] and from Albert et al. (2007) and Grube (2007). The observations of the Cherenkov telescopes are quasi-simultaneous. The best coordination of the Mrk 501 observations with different Cherenkov telescopes was achieved during the observations of its high state in 1997 at VHE—within one day. Furthermore, the difference between the measurements also stems from the fact that they were carried out in different energy ranges (shown in the upper right corner of the figure). Note that the flux from Mrk 501 during its flares increased by more than an order of magnitude. For example, during the April 30–May 1 2009 observations by the VERITAS Collaboration at energies above 300 GeV the flux from this object was 1.8×10^{-10} photon cm^{-2} s^{-1} (Huang and Konopelko 2009), with the object's enhanced activity in 1997 having been confirmed both at VHE and in X rays (2–10 keV). For example, for energies >1 TeV the flux in 1997 exceeded the mean flux over all years of GT-48 observations by a factor of 3.1. A high activity at VHE was recorded with the Whipple, HEGRA, and CAT telescopes. At the same time, the flux in the 2–10 keV band (RXTE/ASM) exceeded its mean value by more than a factor of 6.

To find a possible periodicity in the Swift/BAT, Fermi LAT, and AZT-8 data, we applied the Lomb–Scargle (LS) method (Lomb 1976; Scargle 1982). However, our analysis revealed no period in these energy ranges.

In addition, we constructed a TeV spectrum for Mrk 501 from the GT-48 observations (Fig. 6). The spectral index was 2.0 ± 0.1, which is consistent with the results of the H.E.S.S. Collaboration; according to its data, the spectral index for Mrk 501 changes from 1.9 (high state) to 2.3 (low state) (Cologna et al. 2016). The confidence interval for the H.E.S.S. and GT-48 spectra for Mrk 501 is 95%.

[3] https://cass.ucsd.edu/~rxteagn/Mkn501/Mkn501.html

[4] https://swift.gsfc.nasa.gov/results/transients/weak/Mrk501

[5] https://heasarc.gsfc.nasa.gov/W3Browse/fermi/fermilasp.html

[6] http://veritas.sao.arizona.edu/documents/summarymrk501.table

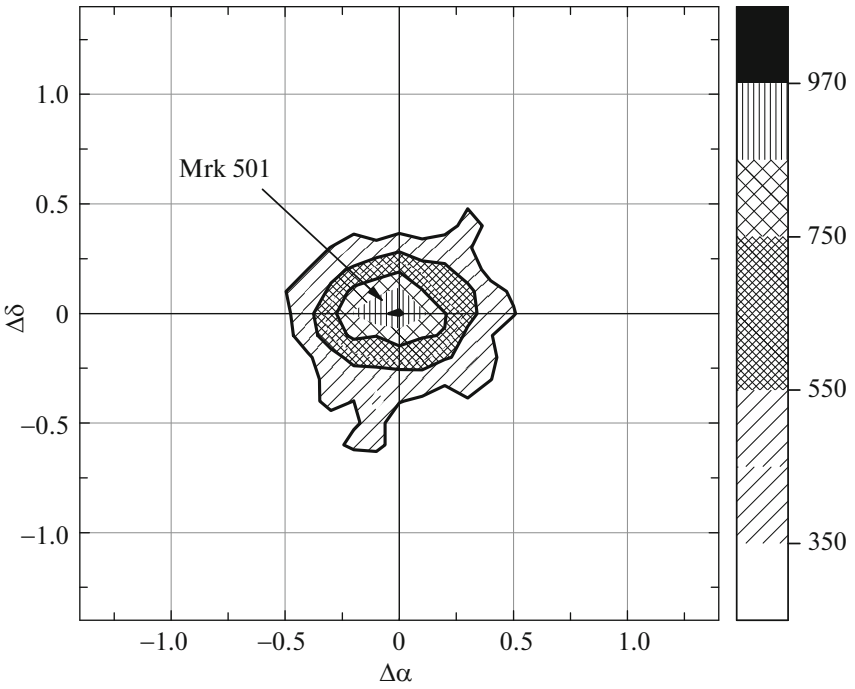

Fig. 4. Localization isophotes for the gamma-ray source Mrk 501. The numbers of events are shown in the upper right corner. The maximum coincides with the position of Mrk 501.

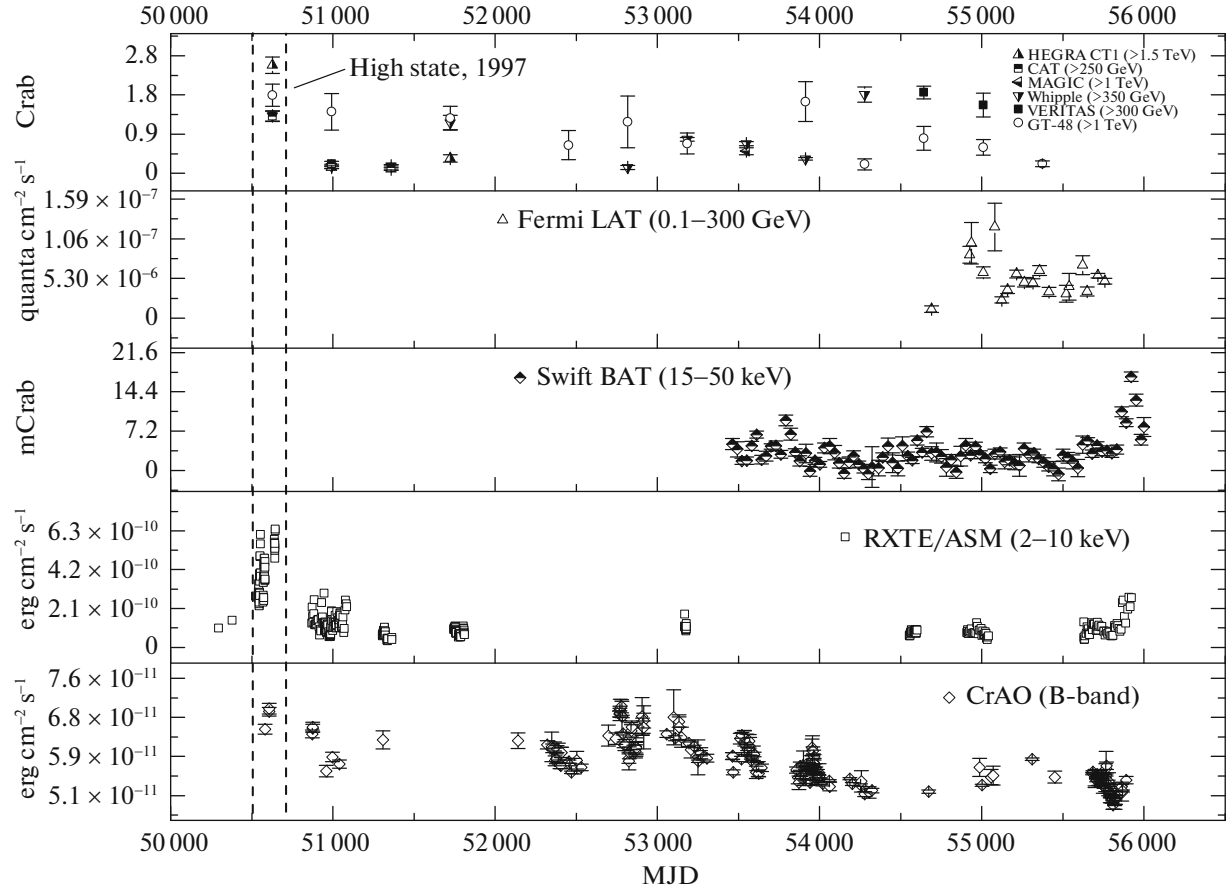

Fig. 5. Fluxes from Mrk 501 in various ranges. The VHE data (upper panel) were normalized to 1 Crab for energies >1 TeV (1 C. U. $= 1.75 \times 10^{-11}$ photon cm^{-2} s^{-1}). The energies at which the observations with the Cherenkov telescopes were carried out are shown in the upper right corner. The Swift/BAT data (the third panel from above) were normalized to mCrab. The conversion factor is 1 mCrab $= 0.00022$ count cm^{-2} s^{-1} (Krimm et al. 2013).

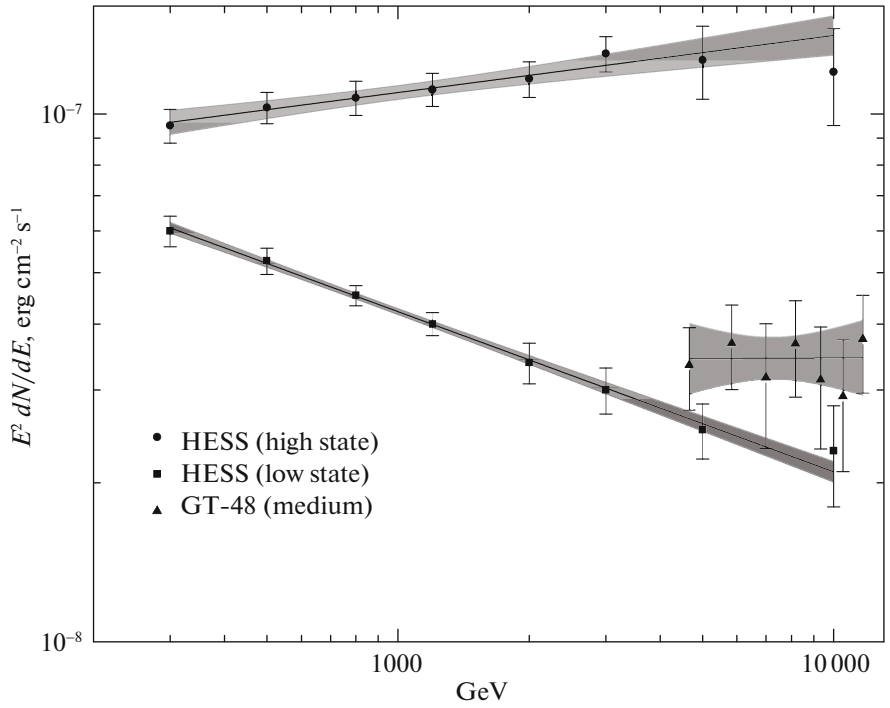

Fig. 6. TeV spectrum of Mrk 501 (for details, see the text). The confidence interval is 95%.

5. CONCLUSIONS

Our observations of the AGN Mrk 501 with the GT-48 Cherenkov telescope from 1997 to 2010 at energies $\geq$1 TeV showed that this object is a VHE gamma-ray source. Large statistics of observations for this object has been accumulated at CrAO over a long period. The total time of Mrk 501 observations over 11 years is more than 180 h. VHE gamma-ray photons were recorded from Mrk 501 with a total significance of 15σ. The GT-48 data have shown for the first time that over such a long time interval ($\sim$14 years) the yearly mean fluxes from this object (over the periods of observations in each year with GT-48) at energies $\geq$1 TeV changed significantly relative to one another (by a factor of 9). Such a result has not been obtained with any other Cherenkov telescope.

According to present views, the matter in AGN jets moves with relativistic speeds and shock waves emerge inside them, which creates conditions for the acceleration of particles to very high energies (for example, the first-order Fermi mechanism, Fermi 1949). The particle composition can be hadronic or leptonic, depending on the AGN jet models, which also affects the VHE gamma-ray production mechanism. In the case of hadronic models, the particles responsible for the gamma-ray production are protons. Accelerating in the jet, the protons gain a colossal energy (up to $\sim 10^{20}$ eV) and then, during the proton–proton or proton–photon interactions followed by an electromagnetic cascade, produce hard gamma-ray emission. In the leptonic model the generation of VHE gamma-ray photons is associated with the inverse Compton scattering of ultrarelativistic electrons. The scattering of accelerated particles by intrinsic synchrotron photons (synchrotron self-Comptonization) is a variety of this mechanism. This mechanism is believed by Abdo et al. (2011) to underlie the formation of the spectral energy distribution for Mrk 501 up to VHE gamma rays. In this scenario the emission is generated in one spherical zone (blob) with a size of $R \sim 10^{17}$ cm. This explains the high variability of objects like Mrk 501, because the variability time scale is related to the Doppler factor and the size of the emission region as

$$t_{\rm var} \simeq \frac{(1+z)R}{c\,\delta}, \qquad (4)$$

where z is the redshift, c is the speed of light, and δ is the Doppler factor.

Accordingly, the variability, including that during the 1997 flare that was also observed with GT-48, can be explained in terms of the models being discussed.

The object Mrk 501 was also observed in other ranges, in particular, at high energies (MeV and GeV) and in the X-ray and optical bands of electromagnetic waves. In some periods a sharp increase in the fluxes occurred synchronously in these ranges. For example, the growth of Mrk 501 activity in 1997

in the entire electromagnetic range was among the most significant ones in the entire history of observations for objects of this subclass. However, the greatest growth was recorded in the VHE range. In this case, an analysis of the data series by the LS method in the optical, X-ray, and gamma-ray bands did not reveal any period in them. No correlation was found between the data series at Fermi energies and in the X-ray range 15–50 keV. Apart from our analysis of the light curves, we constructed a TeV spectrum based on the GT-48 data and determined the differential spectral index (2.0 ± 0.1), which is consistent with the results obtained by the H.E.S.S. Collaboration for TeV energies.

The observations of Mrk 501 and other BL Lac objects are needed to obtain information about the least-studied range of electromagnetic radiation from these extreme objects and to answer the question of particle acceleration, which has not been completely studied and requires additional studies.

ACKNOWLEDGMENTS

We thank S.G. Sergeev for useful discussions and comments to the paper.

REFERENCES

1. A. A. Abdo, M. Akermann, M. Ajello, A. Allafort, L. Baldini, J. Ballet, G. Barbiellini, M. G. Baring, et al., Astrophys. J. **727**, 129 (2011).
2. C. W. Akerlof, M. F. Cawley, M. Chantell, D. J. Fegan, K. Harris, A. M. Hillas, D. G. Jennings, R. C. Lamb, et al., Astrophys. J. Lett. **377**, 97 (1991).
3. J. Albert, E. Aliu, H. Anderhub, P. Antoranz, A. Armada, C. Baixeras, J. A. Barrio, H. Bartko, et al., Astrophys. J. **669**, 862 (2007).
4. J. Aleksic, S. Ansoldi, L. A. Antonelli, P. Antoranz, A. Babic, P. Bangale, U. Barres de Almeida, et al., Astron. Astrophys. **573**, A50 (2015).
5. G. Cologna et al., arXiv:1611.03983v1 (2016).
6. E. Fermi, Phys. Rev. **75**, 1169 (1949).
7. V. P. Fomin, S. Fennell, R. C. Lamb, D. A. Lewis, M. Punch, and T. C. Weekes, Astropart. Phys. **2**, 151 (1994).
8. J. Grube, PhD Thesis (Univ. Leeds, UK, 2007).
9. D. H. Huang and A. Konopelko, arxiv:0912.3772 (2009).
10. O. R. Kalekin, Yu. I. Neshpor, A. A. Stepanyan, et al., Astron. Lett. **21**, 163 (1995).
11. O. R. Kalekin et al., Bull. Russ. Acad. Sci.: Phys. **63**, 606 (1999).
12. H. A. Krimm, S. T. Holland, P. H. D. Corbet, A. B. Pearlman, P. Romano, J. A. Kennea, J. S. Bloom, S. D. Barthelmy, et al., Astrophys. J. Suppl. Ser. **209**, 14 (2013).
13. Ti-Pei Li and Yu-Qian Ma, Astrophys. J. **272**, 317 (1983).
14. N. R. Lomb, Astrophys. Space Sci. **39**, 447 (1976).
15. Yu. I. Neshpor, A. P. Kornienko, and A. A. Stepanian, Exp. Astron. **5**, 405 (1994).
16. J. Quinn, C. W. Akerlof, S. D. Biller, J. Buckley, D. A. Carter-Lewis, M. F. Cawley, M. Catanese, V. Connaughton, et al., Astrophys. J. **456**, L83 (1996).
17. J. D. Scargle, Astrophys. J. **263**, 835 (1982).
18. B. M. Vladimirskii, Yu. L. Zyskin, A. P. Kornienko, Yu. I. Neshpor, A. A. Stepanian, V. P. Fomin, and V. G. Shitov, Bull. Crimean Astrophys. Observ. **91**, 60 (1995).

Translated by V. Astakhov